

Are your MRI contrast agents cost-effective?

Learn more about generic Gadolinium-Based Contrast Agents.



**FRESENIUS
KABI**

caring for life

AJNR

**Improved Detection of Intraventricular
Cysticercal Cysts with the Use of
Three-dimensional Constructive Interference in
Steady State MR Sequences**

Srikanth Subbamma Govindappa, Jayakumar Peruvamba
Narayanan, Vasudev Mandapati Krishnamoorthy, Chandrashekar
Hoskote Shankar Shastry, Anandh Balasubramaniam and Shankar
Susarla Krishna

This information is current as
of April 16, 2024.

AJNR Am J Neuroradiol 2000, 21 (4) 679-684

<http://www.ajnr.org/content/21/4/679>

Improved Detection of Intraventricular Cysticercal Cysts with the Use of Three-dimensional Constructive Interference in Steady State MR Sequences

Srikanth Subbamma Govindappa, Jayakumar Peruvamba Narayanan, Vasudev Mandapati Krishnamoorthy, Chandrashekar Hoskote Shankar Shastri, Anandh Balasubramaniam, and Shankar Susarla Krishna

BACKGROUND AND PURPOSE: Before the advent of MR imaging, intraventricular cysts were difficult to diagnose noninvasively. Among the invasive procedures used were contrast ventriculography and CT ventriculography. MR imaging, with its multiplanar imaging capabilities, excellent depiction of tissue contrast, and versatile parameters, is an important tool in the assessment of intraventricular cystic lesions. We investigated the role of three-dimensional constructive interference in steady state (3D-CISS) MR sequences in the evaluation of intraventricular cysticercal cysts.

METHODS: The study group comprised 11 patients with intraventricular cysticercal cysts. MR studies included spin-echo (SE) T1-weighted, turbo-SE T2-weighted, and 3D-CISS sequences. All images were obtained on a superconducting 1.5-T MR unit. The routine and 3D-CISS sequences were reviewed and interpreted separately by two neuroradiologists.

RESULTS: All patients underwent surgery for excision of intraventricular cysticercal cysts. Eight patients had cysts in the fourth ventricle, two in the lateral ventricle, and one in the third ventricle. SE T1-weighted images showed the cystic wall in nine cases, the scolex in four, and the cystic fluid in two. Turbo-SE T2-weighted images showed the cystic wall and scolex in three and four cases, respectively. The routine sequences did not show the scolex, cystic wall, or cystic fluid together in any of the 11 patients. 3D-CISS images showed the scolex in all 11 patients and the cystic wall and cystic fluid in eight patients each. In seven of the 11 patients, 3D-CISS images showed the scolex, cystic wall, and fluid together.

CONCLUSION: The 3D-CISS sequence is more sensitive and specific than routine SE sequences in the diagnosis of intraventricular cysticercal cysts.

Neurocysticercosis is endemic in developing countries, and patients present with a variety of manifestations. Cysts can be encountered in the parenchyma, ventricles, cisternal spaces, or in several locations at once. Intraventricular cysts cause hydrocephalus and are potentially fatal; they are not always amenable to medical management, and require surgical intervention either for removal or CSF shunting. Before the advent of MR imaging, intraventricular cysts were difficult to diagnose noninvasively. Among the invasive procedures used were contrast ventriculography and CT ven-

triculography. MR imaging, with its multiplanar imaging capabilities, excellent depiction of tissue contrast, and versatile parameters, has made the diagnosis of intraventricular cysticercal cysts easy (1-3). There, however, have been reports of missed intraventricular cysticercal cysts on MR studies in which only routine SE sequences were used (4). Similarly, in our experience, routine MR sequences failed to delineate all the features of an intraventricular cysticercal cyst, necessitating invasive procedures in two patients. A limitation of the standard spin-echo (SE) technique is that it requires relatively thick sections (3 mm). Moreover, the long acquisition time for high-resolution SE T1- and T2-weighted sequences leads to image degradation related to increased patient motion and signal loss (5). This prompted us to investigate the use of an MR technique that is relatively easy, with higher resolution and quicker acquisition times than routine sequences. One such technique is three-dimensional constructive interference in steady state (3D-CISS), a heavily T2-weighted high-resolution

Received May 3, 1999; accepted after revision October 21.

From the Departments of Neuroimaging and Interventional Radiology (S.S.G., J.P.N., V.M.K., C.H.S.S.), Neurosurgery (A.B.), and Neuropathology (S.S.K.), National Institute of Mental Health and Neuro Sciences, Bangalore, India.

Address reprint requests to Dr. S. G. Srikanth, Department of Neuroimaging and Interventional Radiology, National Institute of Mental Health and Neuro Sciences, Bangalore-560 029, India

sequence that has proved useful in the evaluation of cerebellopontine angle lesions and middle and inner ear structures (6). We used this sequence to study our patient population.

Methods

Our study group included seven male and four female subjects, ranging in age from 15 to 45 years. All the patients presented with headache and vomiting, suggesting raised intracranial pressure. In addition, one patient had diplopia and another had blurring of vision. All the patients underwent CT examinations, which revealed obstructive hydrocephalus, prompting withholding of lumbar puncture. Subsequently, all patients were examined with both routine and 3D-CISS MR imaging sequences performed on a 1.5-T superconducting unit. Routine MR sequences included SE T1-weighted and turbo-SE T2-weighted images, obtained in axial, coronal, and sagittal planes. The section thickness was 3 to 5 mm, and the intersection distance was 2 mm. Parameters for the SE T1-weighted images were 350–966/12–14 (TR/TE), a field of view (FOV) of 180–250 mm, and a matrix of 192–256 × 256. Parameters for the turbo-SE T2-weighted images were 3710–3800/90–100, an FOV of 173–240 mm, and a matrix of 192–230 × 256. The routine sequences were reviewed, and regions suggestive of intraventricular cyst were further defined by the 3D-CISS sequence, which had parameters of 12.3/5.9, an FOV of 193 mm, and a matrix of 269 × 512; the slab thickness was 64 mm with 64 partitions, resulting in an effective thickness of 1 mm. Total acquisition time for the routine T1- and T2-weighted sequences was approximately 2 minutes 2 seconds to 3 minutes 4 seconds; for the 3D-CISS sequence, acquisition time was approximately 4 minutes 3 seconds to 6 minutes 1 second.

Images from both the conventional and 3D-CISS sequences were reviewed and interpreted separately by two neuroradiologists. Visibility of the cystic wall, scolex, and cystic fluid were specifically noted. Final decisions were reached by consensus. All patients underwent surgery for excision of the cysts, and histopathologic examination confirmed the diagnosis in each case.

Results

Eight patients had cysts in the fourth ventricle, two in the lateral ventricle, and one in the third ventricle. The presence of cysticercal cysts on MR images was determined specifically by the identification of either the cystic wall, scolex, or cystic fluid. Among the 11 patients, SE T1-weighted images showed the cystic wall in nine, the scolex in four, and the cystic fluid in two. Turbo-SE T2-weighted imaging was sensitive in identifying the cystic wall in three patients and the scolex in four patients. The routine sequences, however, did not show the scolex, cystic wall, and cystic fluid together in any of the 11 patients. The 3D-CISS images showed the scolex in all 11 patients and the cystic wall and fluid in eight patients each; the cystic wall, cystic fluid, and scolex were seen together in seven patients. In three patients, the 3D-CISS did not show either the cystic fluid or the wall. At surgery, the cysts in these three patients were collapsed; nevertheless, they produced obstructive hydrocephalus and therefore were excised.

Discussion

The differential diagnosis of an intraventricular cyst includes choroid plexus cyst, ependymal cyst, colloid cyst, and cysticercal cyst. Choroid plexus cysts are usually asymptomatic and commonly located in the posterolateral ventricles. Ependymal cysts usually occur in the frontal horns of the lateral ventricles and are usually asymptomatic unless they obstruct the foramen of Monro. Colloid cysts are commonly encountered at the roof of the third ventricle, sometimes causing acute hydrocephalus and, rarely, death.

Neurocysticercosis, an infestation by the larval form of pork tapeworm (*Taenia solium*), is the most frequent and widely disseminated human neuroparasitosis; it is endemic in many parts of the world, particularly Latin America, Africa, and Asia. Humans act as intermediary hosts after ingestion of mature, viable *T. solium* eggs via the fecal-oral route. The cysticercal cysts may be encountered in the parenchyma, ventricles, or basal cisterns, or in combined locations. Neurocysticercosis may be asymptomatic or cause varied clinical symptomatology, such as seizures, raised intracranial pressure, ischemic cerebrovascular disease, dementia, and signs of spinal cord compression (7). These are determined by the number of cysts, their location (parenchymal or ventricular), their stage of evolution, and the intensity of the host's immunoinflammatory response. By and large, parenchymal cysticercosis causes seizures, whereas intraventricular cysticercal cysts cause hydrocephalus. In the present series, all the patients had obstructive hydrocephalus.

Intraventricular cysticercal cysts constitute 7% to 20% of neurocysticercosis infections (8), but the frequency may be as high as 33% (9). They are potentially fatal, with death resulting primarily from acute hydrocephalus (10). Although the cysts are encountered in the lateral, third, and fourth ventricles, the fourth ventricle is the most common site of involvement (11, 12), as it was in the present series. They may degenerate, inciting an ependymal reaction that can be identified on contrast-enhanced MR images, leading to permanent neurologic complications (13). Cysticercal cysts in the fourth ventricle may cause mass effect and result in herniation (14).

Until recently, the diagnosis of neurocysticercosis has been supported by cranial CT findings and immunodiagnostic assays of CSF. With the advent of MR imaging, diagnosis has become easier, particularly in the ventricular locations (1, 2). MR imaging is not only superior to CT but is also diagnostic in many CNS parasitic infestations, including neurocysticercosis (15).

A typical cysticercal cyst measures about 8 to 20 mm and surrounds an elongated structure, the scolex, which is fixed at one end and measures 6 × 3 mm (16). Chi-Shing-Zee et al (11) argue that the various stages of evolution of a cysticercal cyst can be differentiated on imaging studies. Clear fluid

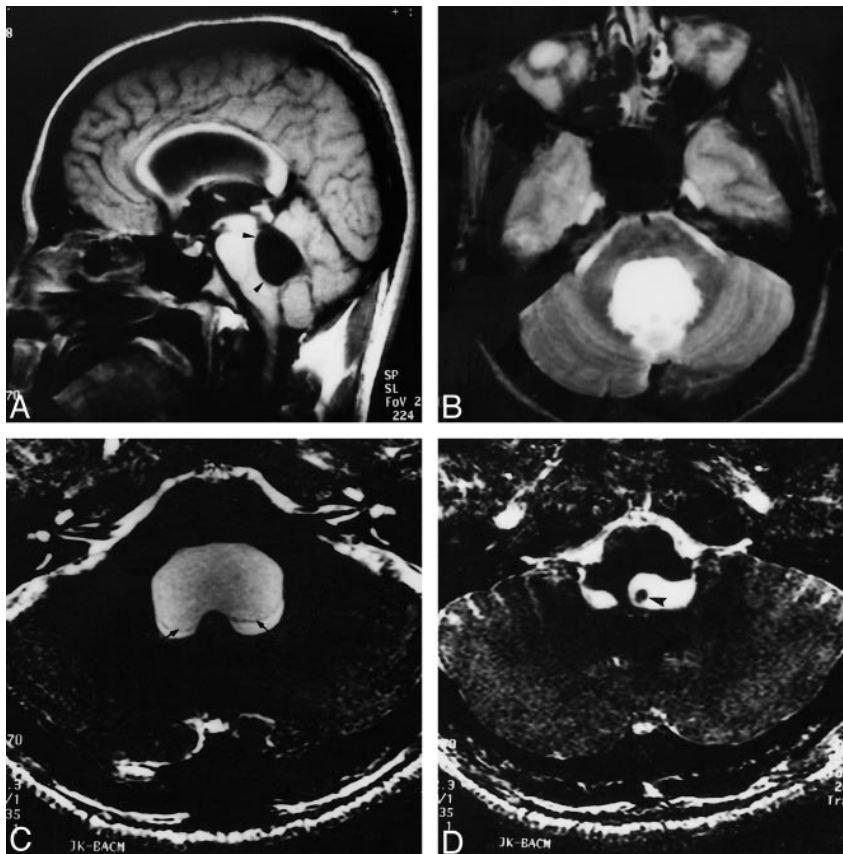


FIG 1. A and B, Sagittal SE T1-weighted (650/14/1) (A) and axial T2-weighted (3800/90/2) (B) images show a dilated fourth ventricle (arrowheads). No cyst is seen.

C and D, Axial 3D-CISS (12.3/5.9/1) images show the cystic wall (arrows) and hypointense scolex (arrowhead).

with an unidentifiable cystic wall can be seen in stage 1. With aging, the parasite develops a thickened wall, which is also identifiable on imaging studies. In addition, the cystic fluid becomes more turbid because of proteinaceous content, which can also be appreciated on MR images. Fluid in apparently live cysts has MR signal properties closely paralleling CSF (2); however, cysts presumed to be degenerated have increased signal intensity on T1-weighted images (12, 17). Thus, the MR characteristics of neurocysticercosis are variable and depend on the stage of evolution of the cyst and its location (15). Typically, the contents of the cyst are hypointense on short-TR/TE images in the majority of lesions, and the scolex is usually isointense with brain (11, 16). On long-TR/TE images, the contents become hyperintense, with loss of internal structural details.

All the patients in our series underwent both routine SE T1-weighted and turbo-SE T2-weighted MR imaging as well as 3D-CISS examination. The majority of intraventricular cysticercal cysts contained hypointense contents on short-TR/TE images (Figs 1 and 2). On long-TR/TE images, the contents were isointense with surrounding CSF, and the lesions were thus obscured (Figs 1 and 2). Earlier investigators encountered similar difficulty in trying to identify intraventricular cysticercal cysts with routine SE T1- and T2-weighted imaging owing to the isointensity of the lesions with surround-

ing CSF (8, 12, 18). There have also been reports of missed intraventricular cysticercal cysts on routine MR images (4). A limitation inherent in the standard 2D Fourier transform SE T1- and T2-weighted techniques is the relatively thick sections (3 mm). Previous authors have observed that the short-TR/TE technique is relatively T1-weighted and not optimal for imaging fluid-filled structures, such as the otic capsule, and long-TR/TE T2-weighted SE MR techniques have limited signal-to-noise ratios. High-resolution standard SE techniques with long acquisition times contribute to image degradation related to increased patient motion and signal loss (5). Hence, we attempted to use the 3D-CISS technique, a high-resolution and heavily T2-weighted MR sequence.

3D-CISS is routinely used in the evaluation of cerebellopontine angle lesions and inner and middle ear structures and epidermoids (6, 19). The millimeter-thin sections, short TE (limited signal loss resulting from magnetic susceptibility effects), and low flip angle (limited T1 weighting) available in this technique allow superb spatial resolution and signal-to-noise ratio within a clinically feasible acquisition time (5). The CISS sequence was originally designed for MR myelography and MR cisternography. It is comparable to the fast imaging in steady-state precision (FISP) sequence (19); however, it is superior to the FISP sequence in reducing the artifacts caused by magnetic field in-

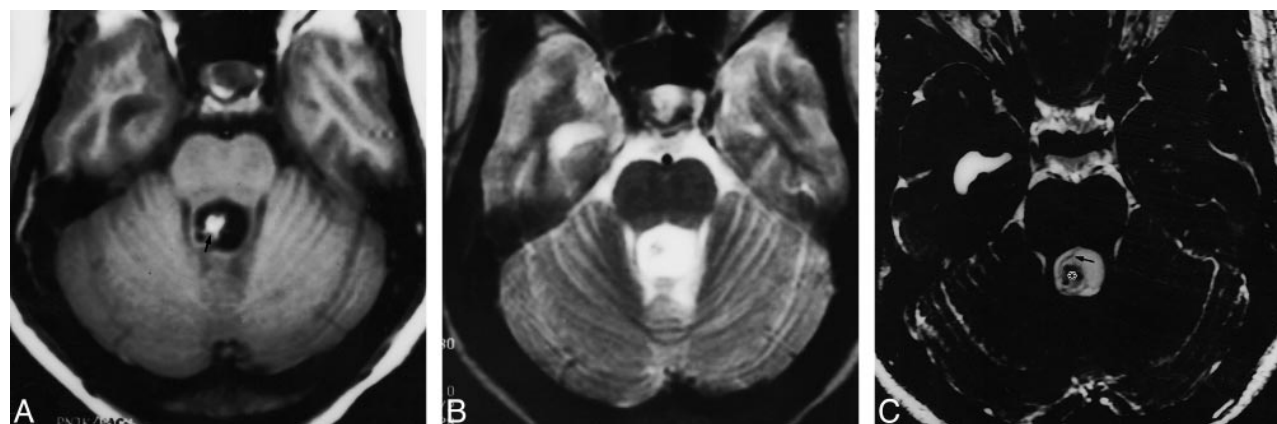


FIG 2. A, Axial T1-weighted (650/14/1) image shows dilatation and distortion of the fourth ventricle with a hyperintense scolex (arrow). B, On T2-weighted (3800/90/2) image, the internal details of the lesion are obscured by the surrounding hyperintense CSF. C, Axial 3D-CISS (12.3/5.9/1) image shows a dilated fourth ventricle, within which the scolices (asterisk) and wall (arrow) of the cyst are clearly seen.

Visibility of intraventricular cysticercosis on three MR imaging sequences

Patient No.	MR Sequence		
	SE T1-weighted	Turbo-SE T2-Weighted	3D-CISS
1	+	—	++
2	+	—	++
3	+	—	++
4	—	+	++
5	+	+	++
6	+	+	++
7	++	+	++
8	+	+	++
9	+	+	++
10	+	+	++
11	+	+	++

Note.—SE indicates spin-echo; 3D-CISS, three-dimensional construction interference in steady state; +, just seen; ++, well seen; —, not seen.

homogeneities. The different sensitivities of the various MR sequences in identifying cysticercal cysts in our patients are given in the Table. Among the 11 patients in our series, the SE T1-weighted images showed the cystic wall in nine, the scolex in four, and the cystic fluid in two. The turbo-SE T2-weighted images were sensitive in identifying the cystic wall in three patients and the scolex in four. In an earlier series, in which MR imaging was used to assess 18 intraventricular cysticercal cysts in 50 patients, T1-weighted images revealed the cystic wall in nine of 22 patients, the scolex in six of 22, and the cystic fluid in five of 22; the T2-weighted images failed to show the cystic wall or scolex in the majority of patients (11). The increased sensitivity of SE T1-weighted images in identifying the features of a cysticercal cyst in our study as compared with the above series was probably the result of the higher strength of our equipment.

In our study, T2-weighted images also failed to show intraventricular cysts in the majority of cases. The 3D-CISS sequence revealed the scolex in all 11 patients and the cystic wall and cystic fluid in eight patients each (Figs 1–3). In seven of 11 patients, the 3D-CISS images showed the cystic wall, cystic fluid, and scolex together. All the patients in our series underwent surgery to remove the cysts; and, in all cases, histopathologic examination confirmed the diagnosis (Fig 4).

Intraventricular cysticercal cysts are associated with a poor prognosis and are potentially fatal (9, 10). They are not always amenable to medical management, and require surgical intervention, either for cyst removal or CSF shunting. Martinez et al (3) advocated a trial of albendazole for patients with cysts in the lateral ventricles and surgical removal for patients with cysts in the third and fourth ventricles. Others, like Cuëtter et al (9), have advocated anthelmintic treatment with albendazole in all cases of intraventricular cysticercal cysts; however, it was necessary to follow up these patients for development of hydrocephalus when shunt surgeries were indicated. Surgical excision is the treatment of choice recommended by many authors (13, 20) before the cyst degenerates and incites ependymal reaction. Ependymitis is a relative contraindication for surgical removal of the cysts and can be identified on contrast-enhanced MR images (10). In the three patients in our series in whom the cystic fluid and wall were not visible on 3D-CISS sequences, the cysts were found to be collapsed at surgery. These cysts were hyperintense on SE T1-weighted images and hypointense on turbo-SE T2-weighted images. These three patients underwent endoscopic ventriculostomy for hydrocephalus and excision of the cysts.

The increased sensitivity of the 3D-CISS sequence is a consequence of its higher resolution and may also be related to accentuation of the T2 value between the cystic fluid and surrounding CSF.

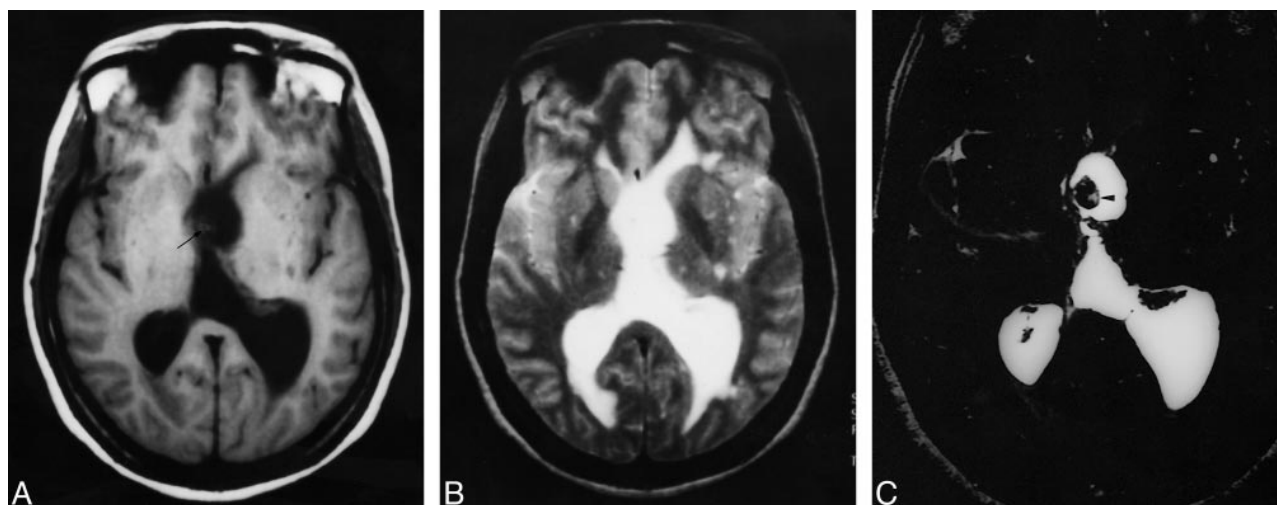


FIG 3. A, Axial T1-weighted (650/14/1) image shows dilatation of the left lateral ventricle with subtle isointense lesion noted in the region of the foramen of Monro (arrow).

B, On T2-weighted (3800/90/2) image, these findings are obscured.

C, Axial 3D-CISS (12.3/5.9/1) image shows the cysticercal lesion more precisely (arrowhead).

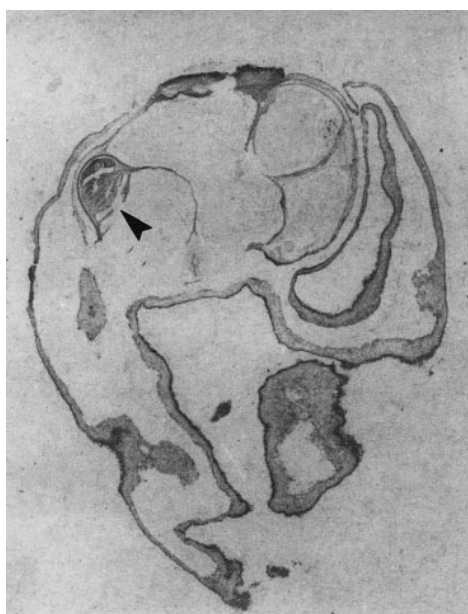


FIG 4. Whole-mount picture of the cysticercal cyst (arrowhead indicates the scolex). Note irregular invaginations of the cyst (hematoxylin-eosin, original magnification $\times 30$).

This has been discussed by other authors in the context of evaluation of epidermoids (19).

Conclusion

Routine SE T1-weighted imaging and turbo-SE T2-weighted imaging were less sensitive than the 3D-CISS technique in the diagnosis of intraventricular cysticercal cysts owing to the poor discrimination between intraventricular cystic fluid and surrounding CSF on the routine imaging sequences.

References

- Martinez HR, Rangel-Guerra RA, Arredondo-Estrado JH, Onofre AMJ. Medical and surgical treatment in neurocysticercosis: a magnetic resonance study of 161 cases. *J Neurol Sci* 1995;130:25–34
- Suss RA, Maravilla KR, Thompson J. MR imaging of intracranial cysticercosis: comparison with CT and anatomopathologic features. *AJNR Am J Neuroradiol* 1986;7:235–242
- Martinez HR, Rangel-Guerra RA, Elizondo G, et al. MR imaging of neurocysticercosis: a study of 56 cases. *AJNR Am J Neuroradiol* 1989;10:1011–1019
- Cudlip SA, Wilkins PR, Marsh HT. Endoscopic removal of a third ventricular cyst. *Br J Neurosurg* 1998;12:452–454
- Brogan M, Chakares DW, Schmalbrock P. High-resolution 3D FT MR imaging of the endolymphatic duct and soft tissues of the otic capsule. *AJNR Am J Neuroradiol* 1991;12:1–11
- Cassleman JW, Kuhweide R, Deimling M, Ampe W, Dehaene I, Meeus L. Constructive interference in steady state (CISS)-3DFT MR imaging of the inner ear and cerebellopontine angle. *AJNR Am J Neuroradiol* 1993;14:47–57
- Pittella JE. Neurocysticercosis. *Brain Pathol* 1997;7:681–693
- Rhee RS, Kumasaki DY, Sarwar M, Rodriguez J, Naseem M. MR imaging of Intraventricular cysticercosis. *J Comput Assist Tomogr* 1987;11:598–601
- Cuether AC, Garcia-Bobadilla J, Guerra LG, Martinez FM, Kaim B. Neurocysticercosis: focus on intraventricular disease. *Clin Infect Dis* 1997;24:157–164
- Zee C-S, Segall HD, Apuzzo ML, Ahmadi J, Dobkin WR. Intraventricular cysticercal cysts: further neuroradiologic observations and neurosurgical implications. *AJNR Am J Neuroradiol* 1984;5:727–730
- Zee C-S, Segall HD, Boswell W, Ahmadi J, Nelson M, Colletti P. MR imaging of neurocysticercosis. *J Comput Assist Tomogr* 1988;12:927–934
- Teitelbaum GP, Otto RJ, Lin M, et al. MR imaging of neurocysticercosis. *AJR Am J Roentgenol* 1989;153:857–866
- Dupplexis E, Dorwling-Carter D, Vidaillet M, Piette JC, Phillippon J. Intraventricular neurocysticercosis: apropos of three cases. *Neurochirurgie* 1988;34:275–279
- McCormick GF. Cysticercosis: review of 230 patients. *Bull Clin Neurosci* 1985;50:76–101
- Chang KH, Han MH. MRI of CNS parasitic diseases. *J Magn Reson Imaging* 1998;8:297–307
- Lotz J, Hewlet R, Alheit B, Bowen R. Neurocysticercosis: correlative pathomorphology and MR imaging. *Neuroradiology* 1988;30:35–41

17. Spickler EM, Lufkin RB, Teresi L, Lanman T, Levesque M, Bentson JR. **High signal intraventricular cysticercosis on T1-weighted MR imaging.** *AJNR Am J Neuroradiol* 1989;10(Suppl): S64
18. Ciftci E, Diaz-Marcham PJ, Hayman LA. **Intradural-extradural spinal cysticercosis: MR imaging findings.** *Comput Med Imaging Graph* 1999;23:161–164
19. Ikushima I, Korogi Y, Hirai T, et al. **MR of epidermoids with a variety of pulse sequences.** *AJNR Am J Neuroradiol* 1997;18: 1359–1363
20. Apuzzo ML, Dobkin WR, Zee C-S, Chan JC, Giannotta SL, Weiss MH. **Surgical considerations in treatment of intraventricular cysticercosis: an analysis of 45 cases.** *J Neurosurg* 1984;60: 400–407